Published in final edited form as:
Neuroimage. 2012 January 16; 59(2): 917–925. doi:10.1016/j.neuroimage.2011.07.035.

Self-modulation of primary motor cortex activity with motor and motor imagery tasks using real-time fMRI-based neurofeedback

Brian D. Berman[1,2], **Silvina G. Horovitz**[2], **Gaurav Venkataraman**[3], and **Mark Hallett**[2]

[1]Department of Neurology, University of Colorado Denver, Denver, CO USA

[2]Human Motor Control Section, National Institute of Neurological Disorders and Stroke (NINDS), National Institutes of Health, Bethesda, MD USA

[3]Reed College, Portland, OR USA

Abstract

Advances in fMRI data acquisition and processing have made it possible to analyze brain activity as rapidly as the images are acquired allowing this information to be fed back to subjects in the scanner. The ability of subjects to learn to volitionally control localized brain activity within motor cortex using such real-time fMRI-based neurofeedback (NF) is actively being investigated as it may have clinical implications for motor rehabilitation after central nervous system injury and brain-computer interfaces. We investigated the ability of fifteen healthy volunteers to use NF to modulate brain activity within the primary motor cortex (M1) during a finger tapping and tapping imagery task. The M1 hand area ROI (ROI_m) was functionally localized during finger tapping and a visual representation of BOLD signal changes within the ROI_m fed back to the subject in the scanner. Surface EMG was used to assess motor output during tapping and ensure no motor activity was present during motor imagery task. Subjects quickly learned to modulate brain activity within their ROI_m during the finger-tapping task, which could be dissociated from the magnitude of the tapping, but did not show a significant increase within the ROI_m during the hand motor imagery task at the group level despite strongly activating a network consistent with the performance of motor imagery. The inability of subjects to modulate M1 proper with motor imagery may reflect an inherent difficulty in activating synapses in this area, with or without NF, since such activation may lead to M1 neuronal output and obligatory muscle activity. Future real-time fMRI-based NF investigations involving motor cortex may benefit from focusing attention on cortical regions other than M1 for feedback training or alternative feedback strategies such as measures of functional connectivity within the motor system.

Keywords

Real-time functional MRI; neurofeedback; finger tapping; motor imagery; primary motor cortex; electromyography

Correspondence: Brian D. Berman, M.D., M.S., University of Colorado Denver, Department of Neurology, 12631 E. 17th Avenue, Mail Stop B-185, Aurora, CO 80045, brian.berman@ucdenver.edu Office: 303-724-2194, Fax: 303-724-2212.

1. Introduction

Technological advances in functional magnetic resonance imaging (fMRI) data processing have made it possible to analyze neural activity as measured by changes in blood-oxygen level dependent (BOLD) contrast almost as quickly as images are acquired allowing for online data monitoring and monitoring of behavioral responses and task performance during a fMRI study (deCharms, 2007; Weiskopf et al., 2007). These real-time fMRI (rtfMRI) capabilities have fostered a wave of exciting new experiments where rapidly updated information of localized brain activity is fed back to the subject in the MRI scanner in order to allow the subject to use this information to learn to voluntarily modulate their own brain activity.

A number of researchers have begun to explore the ability of subjects to use this rtfMRI-guided neurofeedback (NF) to learn how to self-modulate localized brain activity in the scanner environment. Several studies to date have reported that healthy subjects can quickly learn through operant training to use rtfMRI-NF to volitionally control their own brain activity as measured by changes in BOLD signal magnitude in a variety of brain regions. It has been reported that subjects were able to trained to modulate activity in higher cognitive areas such as the amygdala (Posse et al., 2003), inferior frontal gyrus (IFG) (Rota et al., 2008), anterior cingulate cortex (ACC) (deCharms et al., 2005), and insular cortex (Caria et al., 2007).

RtfMRI-NF has also been used to test whether subjects can learn to modulate activation within motor-associated regions using simple motor and motor imagery feedback tasks. One early study using these techniques showed that five healthy volunteers were able to use feedback of their own functional brain maps in hand motor area to adapt finger movement strategies that would lead to a 3-fold number of activated pixels in motor and somatosensory regions, even with about a 60 second delay (Yoo and Jolesz, 2002). In an exploration of the use of rtfMRI-based brain-computer interface (BCI), three healthy volunteers after a brief practice were successfully taught four types of mental tasks that drove a cursor on a two-dimensional maze in different directions (Yoo et al., 2004). These subjects were reported to be able to use NF to increase activity in their sensorimotor cortex during left and right hand motor imagery tasks to accurately move the cursor left and right, respectively.

In an rtfMRI-NF study of nine healthy volunteers by deCharms and colleagues, subjects demonstrated the ability to significantly increase activity in a ROI placed on the margins of the central sulcus that included primary motor and sensory cortex during three 20-minute NF training sessions using finger and hand movement imagery (deCharms et al., 2004). These subjects also maintained the ability to increase activation within this ROI with a motor imagery task immediately after their NF training sessions in a post-training assessment when the NF information was withheld. Expanding on this work, Yoo and colleagues found that rtfMRI-NF was effective in training subjects how to increase the cortical activity within their left primary motor cortex using a right hand movement imagery task and that this ability was retained when retested after a two-week period of daily self-practice (Yoo et al., 2008).

The use of rtfMRI-NF in training individuals how to self-modulate motor and motor-associated cortices has been of great interest as the technique may have clinical utility by improving motor functional rehabilitation strategies or helping monitor functional recovery or reorganization after central nervous system injury. NF training of motor regions might also be able to complement BCI applications such as learning to control the movement of artificial prostheses or possibly even be able to enhance motor functioning in healthy individuals. Potential applications as a targeted, noninvasive intervention in central nervous

system diseases that affect the motor system are also beginning to be explored. Successful application of this technologically advanced strategy to these therapeutic goals, however, will require accurate and reproducible identification of proper feedback targets and a better understanding of the patterns of neural activations that are associated with the motor imagery during NF.

Prior rtfMRI-NF studies involving primary motor regions suggest M1 is amenable to NF-assisted training of the ability to self-modulate brain activity within it using motor imagery. Differing technical approaches, however, do not clearly answer whether this ability is due exclusive activations in M1— a brain region tightly linked to motor output, or whether neighboring sensory and/or motor-associated cortical regions during motor imagery tasks are a more contributory factor. This knowledge could help potentially further enhance the effectiveness of this approach and broaden its applications. Thus, our goal in the present study was to explore rtfMRI-based NF training during a simple motor and motor imagery task using a predominantly hand area M1-containing ROI (ROI_m). Based on prior reports of feasibility, we hypothesized that healthy volunteers could quickly learn to increase the activity within their ROI_m using rtfMRI-generated NF during both a finger-tapping motor task and a hand motor imagery task.

2. Materials and methods

2.1 Participants

We studied 15 healthy volunteers, aged 29.7 ±7.9 years (8F, 7M). All subjects had normal neurological examinations and were right-handed by the Edinburgh Handedness Inventory (Oldfield, 1971). The study was approved by the NIH Combined Neuroscience Institutional Review Board, and all participants gave their written informed consent before participation.

Prior to scanning, participants were instructed in how to perform the alternating finger-tapping task involving their right index and middle fingers, and a similar finger-tapping imagery task during which they imagined such movement of their fingers while keeping completely still and being sure not to actually move their fingers or hand. All subjects were given instructions in the same manner and by the same researcher to help keep motor performance similar across subjects. If an adequate feedback response during rtfMRI was not detected by the participant, they were instructed to try increasing the imagined rate or force of finger movements or try imaging moving more of their hand. Participants were further informed of the inherent hemodynamic delay in addition to an approximate 1 s delay required to process imaging data and update the neurofeedback display.

2.2 MRI scanning

Images were acquired with a 3T scanner and 8-channel head coil (GE Signa, Milwaukee, WI, USA). The coil was foam-padded to restrict head motion and improve subject comfort. Functional T2*-weighted images were acquired using gradient echo, echo planar imaging (EPI), and scanning parameters were selected to keep the whole brain volume acquisition time to within one second so that total feedback time of brain activity to subjects in the scanner was kept at a minimum. These were: matrix size = 64 × 64, FOV = 22 cm × 22 cm, TR = 1000 ms (800 ms for first 6 subjects), TE = 30 ms, flip angle = 70°, and bandwidth = 250 kHz. Each run consisted of 17 slices (14 for first 6 subjects) that covered most of the brain except for the cerebellum (3.3×3.3 mm^2 nominal in-plane resolution, 5.0 mm thick slices, 0.5 mm gap). To improve the signal-to-noise ratio in areas prone to susceptibility artifacts, high-order shimming was applied to lessen the field inhomogeneities during data collection. A high-resolution anatomical scan was acquired for each subject for superposition of functional maps upon brain anatomy and to allow for image normalization

to a standardized brain space using a magnetization-prepared rapid gradient echo (MPRAGE) sequence (matrix size = 256 × 256, FOV = 22 cm × 22 cm, 1 mm^3 isotropic resolution, TR = 10 ms, TE = 4.96 ms, flip angle = 19°).

2.3 Real-time fMRI scanning

Functional imaging data was acquired and exported in real-time to a console at the scanner that was running the Analysis of Functional NeuroImages (AFNI) software (Cox, 1996), which allows for real-time motion correction and continuously updated BOLD signal time-course display (Figure 1a). ROI_m was functionally localized during the performance of the first run, which consisted of blocks of self-paced finger tapping alternating with rest. A 16.5 × 16.5 × 5 mm^3 (10 × 10 × 5 mm^3 for first 6 subjects) ROI was placed in the vicinity of the anatomically visualized hand knob region (Yousry et al., 1997) and centered where the maximum BOLD activation changes were able to be visually detected throughout all voxels in the ROI (Figure 1b, see Supplementary Material). A reference (ROI_{ref}) encompassing the entire brain volume in an axial slice distant from ROI_m was used to correct for global scanning effects during the rtfMRI scanning.

The mean BOLD signal within the specified ROIs was extracted and exported in real time to a dedicated Linux workstation. In-house Python routines were developed to read BOLD signal changes and produce a dynamic visual display that conforms to standard block fMRI experimental design. The feedback display consisted of a red column with a height that was continuously updated after an initial baseline rest block at each TR using the following equation:

$$\text{Column height (TR)} = \frac{[\text{ROI}_m(\text{TR})/\text{ROI}_m(\text{baseline})]}{[\text{ROI}_{ref}(\text{TR})/\text{ROI}_{ref}(\text{baseline})]}$$

No thresholds were applied. The feedback display also contains a solid bar at the top to represent the target level of activity, a dashed line representing the average level of activity measured during the baseline rest block, and an arrow to emphasize the direction brain activity is to be modulated (Figure 1c).

2.4 Surface EMG

MRI-compatible surface electromyography (EMG) Ag-AgCl electrodes (BIOPAC Systems, Inc., Goleta, CA, USA) and recording system (Brain Products, Munich, Germany) were used for every subject to detect muscle activity during the tapping and tapping imagery scanning runs and monitor task performance (Figure 1d, see Supplementary Material). One electrode was placed on the right first dorsal interosseous muscle and a reference channel was placed on the dorsum of the right hand. Before starting the scanning run, each subject's tapping waveforms were inspected outside and then inside the scanner room to verify adequate detection of muscle movement. The MRI scanner artifact correction and band-pass filtering were performed on EMG waveforms using the commercially available Brain Products software Vision Analyzer (details provided in the Supplementary Material).

Neurofeedback task paradigm—The two types of tasks during rtfMRI scanning were performed in a block design fashion (Figure 2). Each scan began with 10 s for T1 signal stabilization and participant acclimation to the scanner environment before an initial 20 s baseline rest block. During rest blocks participants saw a fixation cross to indicate rest and were encouraged to relax and think of the letters "A, B, C" or numbers "1, 2, 3" in order to divert their focus from the NF tasks. Counting backward and other numerical operations during the rest period were discouraged because this has been shown to activate a network

that involves regions related to finger movement (Fehr et al., 2007; Hanakawa, 2011). During the "GO" task, participants saw the word "GO" on the screen, instructing them to either tap their fingers in a self-paced manner or perform mental imagery of finger or hand movement. During the feedback ("FB") task, participants were shown a continuously updated feedback display (Figure 1c) and instructed to try and increase the column height toward the goal bar and maintain its height there using either the motor or motor imagery task. Scanning runs consisted of a total of 5 alternating active and rest blocks of 20 seconds each after the initial baseline rest block.

Prior to each rtfMRI scanning run, subjects were verbally reminded of the instructions for the subsequent task condition. The first rtfMRI scanning run was a finger tapping GO run, performed first in order to functionally localize the hand motor region, followed by a finger tapping FB run, a motor imagery GO run, and then 3 FB training motor imagery runs (1 for first 6 subjects). The number of training runs was increased from one to three after 6 subjects because these initial subjects reported in post-scanning assessments that one training motor imagery run was too short and insufficient to be able to assess their performance during the more challenging motor imagery task. The size of ROI_m was increased from at the same time due to concerns that a smaller ROI might be more susceptible to subject movement over the increased number of runs. A final motor imagery GO run—referred to as a "transfer" (XSFR) run—was performed to evaluate if NF training led to an increased ability to modulate brain activity in the ROI_m in the absence of the NF display.

2.5 Image analysis

Functional imaging data were analyzed offline using AFNI (Cox, 1996). The first 10 seconds of each session were excluded from data analysis to account for T1 equilibration effects and subject acclimation. The functional EPI data were then corrected for non-simultaneous slice acquisition and registered to the last EPI scan (closest to anatomical scan acquisition). Images were spatially smoothed using an isotropic 8-mm full width at half-maximum Gaussian filter to accommodate individual anatomical variability. Time series data for each individual were then analyzed using a multiple regression model. For individual subject analysis, task-related changes in BOLD signal were estimated at each voxel using a box-car block-design function convolved with a standard gamma-variate hemodynamic response function and entered as a regressor of interest in the general linear model (GLM). Six motion parameters were also included into the GLM to take into account artifacts caused by head motion. The AFNI program *3dDeconvolve* was used to estimate the voxel-wise response amplitude for the regressor of interest in addition to performing voxel-wise linear contrasts between the individual subject's GO, FB and XSFR runs for the finger-tapping and the motor imagery tasks. Group analysis was performed using a simplified mixed-effects model (one-sample t-test at second level) to test for within-group task-related and contrast-related differences in brain activations. Family-wise error correction for multiple comparisons was performed using Monte Carlo based simulations (AFNI program *AlphaSim*) to calculate cluster sizes that lead to an overall corrected significance level of $p < 0.001$.

2.6 ROI Analysis

Raw BOLD signal time-course data were extracted from each subject's slice-timing and motion corrected EPI scans using their previously defined ROI_m and shifted 5 seconds to account for the hemodynamic delay. The BOLD signal data at each time point (TR) was normalized to the mean BOLD signal within a whole brain mask (created from the individual anatomical MRIs) rather than the single distant brain slice used to correct for global scanning effects during real-time scanning in order to better account for these effects

as well as whole-brain activity effects. Paired, two-tailed t-tests were used to assess for significant changes in the ROIs between the task and rest states with significance level set at $p < 0.05$.

3. Results

3.1 Modulation of ROI_m

All participants completed the finger-tapping and motor imagery NF scanning runs. Using rtfMRI-NF, all subjects were able to successfully increase the magnitude of the BOLD signal within ROI_m during the simple motor finger-tapping task and reach the goal bar. Visual inspection of the BOLD signal changes during the GO and FB runs averaged over all subjects supports that the subjects were able to quickly increase activity in M1 to the goal level and then maintain it through the entire active block (see Supplementary Material). Additionally, no evidence of habituation of M1 activity toward the end of the tapping blocks or runs was seen.

No significant difference (p=0.35) was seen in mean percent signal change within ROI_m between the finger tapping runs with (FB) and without (GO) the presence of NF (Figure 3a). Accordingly, there was no significant difference (p=0.75) in the measured EMG activity levels during tapping between the FB and GO runs. Exploratory analysis of a relationship between the detected BOLD activity within ROI_m and the measured EMG signal for each subject revealed no significant correlation within or across subjects. Investigation of BOLD changes and measured EMG signal in a within subject analysis of the active blocks in the FB runs revealed a significant positive linear relationship (p<0.025) in 7 subjects, a negative relationship (p≤0.025) in 2 subjects, and no significant relationship in the remaining 6 subjects (see Supplementary Material).

Participants were not able to successfully increase BOLD signal within ROI_m during the motor imagery runs regardless if they underwent a single (N=6, p=0.64) or three (N=9, p=0.71) training feedback runs (Figure 3b). There was no significant difference between the single FB run for the first 6 subjects and the first FB run for the 9 subjects with three FB runs (−0.150 +/− 0.434 vs. −0.184 +/− 0.206, p=0.84). The similarity of the BOLD signal changes in these initial runs suggests the change in size of the target ROI did not affect the results. Group-level mean BOLD signal magnitude in the ROI_m suggested a decrease during the GO and FB runs, but the mean signal changes were not significantly different from baseline for any of the motor imagery runs. In addition, there was no difference seen between the first and third FB run in the group with three FB runs (−0.184 +/− 0.206 vs. −0.171 +/− 0.212, p=0.90) arguing against the presence of a training effect. Although group and subgroup analysis revealed no significant findings on a group level, there was a suggestion that some of the subjects may have succeeded in increasing activity within ROI_m during some of the imagery NF runs (see Supplementary Material). Only one subject, however, demonstrated a hypothesized steady increase in ROI_m activity across all imagery NF runs.

Surface EMG during scanning runs showed that the right hand of all participants remained still during motor imagery tasks except for two participants who began to finger tap during a motor imagery run. These scanning runs were immediately stopped and repeated after the subject was reminded that the current task was motor imagery before repeating the run.

3.2 Whole-brain activations during GO and FB tasks

Right handed finger tapping without NF activated primarily motor-associated brain regions including the left hand area M1 and neighboring somatosensory cortex, inferior parietal lobe (IPL), and thalamus (Figure 4a, Table 1). A small region of activation within the

supplementary motor area (SMA)/medial frontal gyrus (MeFG) was present when the significance threshold was lowered to $p < 0.001$, uncorrected. A small cluster of significant deactivation was identified in the right paracentral lobule. In the presence of NF, the finger-tapping task activated the same areas as seen without NF as well as a number of other brain regions including the SMA/MeFG, right premotor cortex (precentral and middle frontal gyrus, MFG), the right intraparietal sulcus (IPS), IPL, superior parietal lobe (SPL), and precuneus, the right IFG, and bilateral middle occipito-temporal cortex (Figure 4b, Table 1).

During tapping imagery without NF, a widespread network of significant activations was seen that included the SMA and ventral ACC, and bilateral premotor cortex, IPL, and putamen (Figure 4c, Table 1). The tapping imagery also activated part of the left MFG corresponding to dorsolateral prefrontal cortex (DLPFC), as well as the left superior frontal gyrus (SFG) and anterior insular cortex. Significant deactivations were identified in the right greater than left precuneus, posterior cingulate cortex and dorsal ACC, in addition to the right primary somatosensory cortex. In the presence of NF, tapping imagery was associated with overlapping areas of activations as seen without NF along with additional activations found within the right IPS and IFG, bilateral SPL and precuneus, bilateral thalamus, and bilateral middle occipito-temporal cortex (Figure 4a, Table 1). The tapping imagery task with NF was further associated with deactivations in the left somatosensory cortex and bilateral posterior insular cortex.

3.3 Contrast analysis

The contrasts of FB versus GO runs for both the finger tapping and tapping imagery tasks revealed significant homologous activations within premotor cortex regions including the precentral gyrus and MFG, right IFG, right IPS and IPL, bilateral SPL and precuneus, right greater than left MTG, and bilateral middle occipital gyrus (MOG) (Figure 5a and 5b, Table 2). Significant activations for the contrasts of FB versus GO were also seen within the right anterior insular cortex during the finger tapping task, and the right thalamus for the tapping imagery task. The contrast of XSFR versus GO for the tapping imagery runs (not displayed) revealed no significant activation differences.

4. Discussion

Subjects in our study were, in a single scanning session, able to incorporate rtfMRI-based NF during a motor finger-tapping task and increase activity within their functionally localized hand area M1. These results are similar to previous studies investigating the use of NF of motor cortex areas during the performance hand motor tasks (deCharms et al., 2004; Yoo and Jolesz, 2002). Not previously reported, however, is an explanation of how the subjects were able to modulate M1 activity during the motor tasks. Since we recorded surface EMG on all subjects during tapping, we investigated the hypothesis that subjects modulate M1 activity during NF by altering hand muscle activity. Of the nine subjects where a significant linear relationship between EMG and BOLD signal existed, seven had a positive relationship signal helping support that increased BOLD was obtained through increased muscle activity during the NF runs. Monitoring of recruited muscles beyond just the first dorsal interosseous during tapping may be needed to more definitively answer if changing the degree of muscle activity is indeed how subjects are able to modulate M1 activity during NF.

During the motor execution runs, a more widespread network of activations was present during the motor FB run, but there was no significant difference between mean levels of BOLD activity within ROI_m during the motor GO and FB runs after correction for whole-brain activity changes. Since there was also no difference across subjects in motor activity as assessed by surface EMG between the GO and FB runs, the additional activations outside

ROI_m during the FB are unlikely the result of motor performance differences between the two task conditions. The additional activations seen during the FB condition are therefore more likely attributable to the recruitment of brain regions involved in visuomotor processing (Caminiti et al., 1996; Cavanna and Trimble, 2006; Culham and Kanwisher, 2001; Ilg and Thier, 2008).

In contrast to previously reported rtfMRI-NF investigations involving motor imagery (deCharms et al., 2004; Yoo et al., 2004; Yoo et al., 2008; Yoo et al., 2007), subjects in our study did not show an ability to selectively modulate brain activity within M1 proper during a hand motor imagery task with or without the use of NF. That motor imagery did not result in an increase in M1 activity in our study may be because M1 activity as measured by fMRI is tightly linked to the amount of actual motor activity and only by changing this activity will M1 neurons be recruited. While a recent review of motor imagery investigations suggests that there is evidence that motor imagery can lead to at least transient activation of M1 (Munzert et al., 2009), whether functional imaging studies have clearly demonstrated that M1 proper is activated during motor imagery tasks remains controversial. Indeed, motor imagery performance appears dependent only on central processing mechanisms and does not require an intact M1 (Lotze and Halsband, 2006; Sirigu et al., 1995), and a number of imaging studies have found no participation of M1 during motor imagery in most of the subjects studied (Binkofski et al., 2000; Dechent et al., 2004; Gerardin et al., 2000; Hanakawa et al., 2008; Hanakawa et al., 2003).

The lack of consistent M1 activation with motor imagery in prior imaging studies, and the failure of subjects in our study to increase activity within their hand area M1 using motor imagery even with the presence of NF, may stem from such activations being isolated to small subdivisions of M1 located more anteriorly to the those neurons activated during motor execution (Sharma et al., 2008). Alternatively, active suppression or inhibition of M1 proper may occur during motor imagery in order for the subject to avoid making an overt movement. In one recent motor system connectivity study, weak and positive influences of premotor cortex, SMA, SPL, and IPS on M1 during motor execution were found to be strong and negative during motor imagery, supporting the presence of a suppressive effect on M1 when overt movements are inhibited (Solodkin et al., 2004). While not significant, our data raises the possibility that motor imagery actually leads to a decrease in BOLD signal in M1 (see Figure 3b), possibly due to this area being actively inhibited when subjects prevent themselves from moving while simultaneously performing imagination of a particular movement. Nevertheless, motor cortex inhibition is correlated with hemodynamic and metabolic down-regulation (Stefanovic et al., 2004), and so would be expected to be associated with a decrease or lack of measurable change in the BOLD signal (Waldvogel et al., 2000). Better characterization of the hemodynamic responses to neural inhibition, however, is still needed (Logothetis, 2008).

A number of imaging studies have demonstrated that a widespread network of brain areas including premotor and somatosensory cortex, as well as the SMA and motor-associated regions within the DLPFC, basal ganglia, ACC, insular cortex, and parietal cortex, are activated during motor imagery (Cavanna and Trimble, 2006; Decety, 1996; Hanakawa et al., 2008; Munzert et al., 2009; Wolbers et al., 2003). The presence of overlapping activations seen during the GO and FB imagery runs with these previously described motor imagery-related activations suggests that subjects in our study were appropriately engaged in motor imagery during the rtfMRI-NF runs. The discrepancy of our results to prior rtfMRI-NF studies involving motor imagery, therefore, may be attributable to differences in target ROI size and placement. In our study, M1 was functionally localized and the ROI included motor cortex clearly activated during finger tapping rather than determined using an automated segmentation method (Yoo et al., 2008). Additionally, our target ROI was

considerable smaller than the 35 mm × 35 mm ROI used by deCharms (deCharms et al., 2004). Although the use of a smaller ROI may increase the potential for confounding effects such as subject movement, our smaller, functionally localized ROI during a hand motor task ensured our ROI contained predominantly M1 cortex and limited the inclusion of neighboring premotor or primary somatosensory cortex. It is possible that the successful modulation of motor cortex in prior earlier rtfMRI-NF studies may be accounted for by the inclusion of neighboring premotor or somatosensory cortex into the NF-targeted primary motor cortex ROI. The well-established premotor cortex activation during motor imagery along with our findings and similar findings demonstrated in prior motor-related rtfMRI-NF studies suggest the premotor cortex may represent a better motor-associated target region for NF training and should be explored in future rtfMRI-NF investigations.

Other methodological and analysis approaches may also help explain our negative findings compared to previous positive findings. First, we did not rely solely on visual monitoring of hand motion (Yoo et al., 2008) and instead used surface EMG to carefully monitor hand motion of every subject as opposed to a few subjects (deCharms et al., 2004) in order to ensure that no movement of the right hand occurred during tapping imagery. In our study, EMG monitoring led to the detection of two subjects who accidentally begin moving during imagery tasks. As small muscle contractions without any obvious overt movement could lead to pronounced BOLD activations in M1 and potentially be falsely attributed to imagery, EMG monitoring during motor imagery tasks is especially important to eliminate this confound. Additionally, our findings are reported as mean percent signal changes normalized to whole-brain activity at each time point in order to account for any non-specific or whole-brain activation changes. This more strictly defines the NF-training results and more accurately reflects whether subjects were able to selectively modulate brain activity within the localized ROI rather than reporting an increase that could be due to a diffuse increase in brain activations during NF scanning. Lastly, if learned modulation M1 proper is feasible with rtfMRI-NF, then the negative findings of our study may be the result of insufficient training. In the motor imagery rtfMRI-NF study by deCharms et al., the approximately 0.25% mean signal increase within the sensorimotor cortex ROI required three 20-minute NF training sessions (deCharms et al., 2004). Thus, more intensive training than that used in our study may be required for subjects to learn to self-modulate M1 using NF.

As highlighted by the contrast analyses of the FB to GO runs, the presence of NF activated a consistent and widespread network during both the motor and motor imagery tasks. This network included the IPS, which is thought to have principal functions related to the dorsal stream pathway of the visual system and could be playing a role in visual attention and directing eye movements during visuomotor coordination tasks (Culham and Kanwisher, 2001), as well as the IPL, SPL and precuneus, which have all been associated with visuospatial attention and processing (Caminiti et al., 1996; Cavanna and Trimble, 2006; Rizzolatti et al., 1998). The activations seen in the MOG and MTG are also consistent with the importance of these areas in the processing of visual motion, which may represent the underlying processing of sustained smooth pursuit eye movement (Ilg and Thier, 2008). The MOG activations may also be explained by recruitment of the extrastriate body area, which has been associated with the limb movements as well as mental motor imagery in response to a visual target stimulus (Astafiev et al., 2004). Since this network was similar for both task types, these parietal and occipito-temporal activations may be related to the NF training itself; however, network activations associated with the process of rtfMRI-NF have not been directly investigated.

To date, rtfMRI-based motor imagery studies have primarily used a targeted motor area ROI for NF training. Incorporating motor-network patterns of activation into rtfMRI studies

rather than a single localized brain region may be a useful approach to improve the effectiveness of NF training with motor imagery tasks. Alternatively, using rtfMRI-NF to train individuals to modulate functional connectivity within the motor network may lead to more effective training could help expand the clinical utility of this technologically advanced methodology. In a preliminary study by our group, the presence of NF during a finger tapping task was found to lead to an increase in M1 functional connectivity to the contralateral M1 (ipsilateral to movement) and bilateral basal ganglia (Horovitz et al., 2010). Further studies are needed to assess whether the presence of NF also has effects on motor network connectivity during motor imagery. Future investigations are also needed to determine if individuals can learn how to self-modulate large-scale motor network activations or the functional connectivity within motor circuits using rtfMRI-NF training.

5. Conclusions

Our findings suggest that while the ability to self-modulate M1 proper using rtfMRI-based NF can be quickly acquired using a simple finger tapping motor task, this was not the case when subjects used a motor imagery task. These results may reflect an inherent limitation of this cortical area to be recruited during motor imagery alone without any overt movement. The discrepancy between our findings and prior reports of successful rtfMRI-based NF learning of the ability to modulate activity in M1 may be related to technical differences such as the inclusion of non-primary motor cortex regions within the localized brain regions used for NF training. Future rtfMRI-NF investigations involving motor imagery might be improved by focusing on alternative motor cortex targets, such as the premotor cortex, or by exploring the ability of subjects to alter motor network connectivity.

Supplementary Material

Refer to Web version on PubMed Central for supplementary material.

Acknowledgments

The Intramural Research Program of the NINDS/NIH supported this research. We are grateful to Jerzy Bodurka for his help in setting up the real-time fMRI functionality used in this study.

Abbreviations

ACC	anterior cingulate cortex
AFNI	Analysis of Functional NeuroImages
BOLD	blood-oxygen level dependent
BCI	brain-computer interface
DLPFC	dorsolateral prefrontal cortex
EMG	electromyography
fMRI	functional magnetic resonance imaging
GLM	general linear model
IFG	inferior frontal gyrus
IPL	inferior parietal lobe
IPS	intraparietal sulcus
M1	primary motor cortex

MeFG	medial frontal gyrus
MFG	middle frontal gyrus
MOG	middle occipital gyrus
NF	neurofeedback
rtfMRI	real-time fMRI
ROI	region of interest
SMA	supplementary motor area
SFG	superior frontal gyrus
SPL	superior parietal lobe

References

Astafiev SV, Stanley CM, Shulman GL, Corbetta M. Extrastriate body area in human occipital cortex responds to the performance of motor actions. Nature Neuroscience. 2004; 7:542–548.

Binkofski F, Amunts K, Stephan KM, Posse S, Schormann T, Freund HJ, Zilles K, Seitz RJ. Broca's region subserves imagery of motion: A combined cytoarchitectonic and fMRI study. Human Brain Mapping. 2000; 11:273–285. [PubMed: 11144756]

Caminiti R, Ferraina S, Johnson PB. The sources of visual information to the primate frontal lobe: A novel role for the superior parietal lobule. Cerebral Cortex. 1996; 6:319–328. [PubMed: 8670660]

Caria A, Veit R, Sitaram R, Lotze M, Weiskopf N, Grodd W, Birbaumer N. Regulation of anterior insular cortex activity using real-time fMRI. Neuroimage. 2007; 35:1238–1246. [PubMed: 17336094]

Cavanna AE, Trimble MR. The precuneus: a review of its functional anatomy and behavioural correlates. Brain. 2006; 129:564–583. [PubMed: 16399806]

Cox RW. AFNI: software for analysis and visualization of functional magnetic resonance neuroimages. Comput Biomed Res. 1996; 29:162–173. [PubMed: 8812068]

Culham JC, Kanwisher NG. Neuroimaging of cognitive functions in human parietal cortex. Current Opinion in Neurobiology. 2001; 11:157–163. [PubMed: 11301234]

Decety J. The neurophysiological basis of motor imagery. Behavioural Brain Research. 1996; 77:45–52. [PubMed: 8762158]

deCharms RC. Reading and controlling human brain activation using real-time functional magnetic resonance imaging. Trends Cogn Sci. 2007; 11:473–481. [PubMed: 17988931]

deCharms RC, Christoff K, Glover GH, Pauly JM, Whitfield S, Gabrieli JD. Learned regulation of spatially localized brain activation using real-time fMRI. Neuroimage. 2004; 21:436–443. [PubMed: 14741680]

deCharms RC, Maeda F, Glover GH, Ludlow D, Pauly JM, Soneji D, Gabrieli JD, Mackey SC. Control over brain activation and pain learned by using real-time functional MRI. Proc Natl Acad Sci U S A. 2005; 102:18626–18631. [PubMed: 16352728]

Dechent P, Merboldt KD, Frahm J. Is the human primary motor cortex involved in motor imagery? Cognitive Brain Research. 2004; 19:138–144. [PubMed: 15019710]

Fehr T, Code C, Herrmann M. Common brain regions underlying different arithmetic operations as revealed by conjunct fMRI-BOLD activation. Brain Research. 2007; 1172:93–102. [PubMed: 17822681]

Gerardin E, Sirigu A, Lehericy S, Poline JB, Gaymard B, Marsault C, Agid Y, Le Bihan D. Partially overlapping neural networks for real and imagined hand movements. Cerebral Cortex. 2000; 10:1093–1104. [PubMed: 11053230]

Hanakawa T. Rostral premotor cortex as a gateway between motor and cognitive networks. Neurosci Res. 2011; 70:144–154. [PubMed: 21382425]

Hanakawa T, Dimyan MA, Hallett M. Motor Planning, Imagery, and Execution in the Distributed Motor Network: A Time-Course Study with Functional MRI. Cereb Cortex. 2008

Hanakawa T, Immisch I, Toma K, Dimyan MA, Van Gelderen P, Hallett M. Functional properties of brain areas associated with motor execution and imagery. J Neurophysiol. 2003; 89:989–1002. [PubMed: 12574475]

Horovitz SG, Berman BD, Hallett M. Real time BOLD functional MRI neuro-feedback affects functional connectivity. Conf Proc IEEE Eng Med Biol Soc. 2010; 1:4270–4273. [PubMed: 21096645]

Ilg UJ, Thier P. The neural basis of smooth pursuit eye movements in the rhesus monkey brain. Brain and Cognition. 2008; 68:229–240. [PubMed: 18835077]

Logothetis NK. What we can do and what we cannot do with fMRI. Nature. 2008; 453:869–878. [PubMed: 18548064]

Lotze M, Halsband U. Motor imagery. Journal of Physiology-Paris. 2006; 99:386–395.

Munzert J, Lorey B, Zentgraf K. Cognitive motor processes: The role of motor imagery in the study of motor representations. Brain Research Reviews. 2009; 60:306–326. [PubMed: 19167426]

Oldfield RC. Assessment and analysis of handedness - Edinburgh inventory. Neuropsychologia. 1971; 9:97–113. [PubMed: 5146491]

Posse S, Fitzgerald D, Gao K, Habel U, Rosenberg D, Moore GJ, Schneider F. Real-time fMRI of temporolimbic regions detects amygdala activation during single-trial self-induced sadness. Neuroimage. 2003; 18:760–768. [PubMed: 12667853]

Rizzolatti G, Luppino G, Matelli M. The organization of the cortical motor system: new concepts. Electroencephalography and Clinical Neurophysiology. 1998; 106:283–296. [PubMed: 9741757]

Rota G, Sitaram R, Veit R, Erb M, Weiskopf N, Dogil G, Birbaumer N. Self-regulation of regional cortical activity using real-time fMRI: The right inferior frontal gyrus and linguistic processing. Hum Brain Mapp. 2008; 30:1605–1614. [PubMed: 18661503]

Sharma N, Jones PS, Carpenter TA, Baron JC. Mapping the involvement of BA 4a and 4p during Motor Imagery. Neuroimage. 2008; 41:92–99. [PubMed: 18358742]

Sirigu A, Cohen L, Duhamel JR, Pillon B, Dubois B, Agid Y, Pierrotdeseilligny C. Congruent unilateral impairments for real and imagined hand movements. Neuroreport. 1995; 6:997–1001. [PubMed: 7632907]

Solodkin A, Hlustik P, Chen EE, Small SL. Fine modulation in network activation during motor execution and motor imagery. Cerebral Cortex. 2004; 14:1246–1255. [PubMed: 15166100]

Stefanovic B, Warnking JM, Pike GB. Hemodynamic and metabolic responses to neuronal inhibition. Neuroimage. 2004; 22:771–778. [PubMed: 15193606]

Waldvogel D, van Gelderen P, Muellbacher W, Ziemann U, Immisch I, Hallett M. The relative metabolic demand of inhibition and excitation. Nature. 2000; 406:995–998. [PubMed: 10984053]

Weiskopf N, Sitaram R, Josephs O, Veit R, Scharnowski F, Goebel R, Birbaumer N, Deichmann R, Mathiak K. Real-time functional magnetic resonance imaging: methods and applications. Magn Reson Imaging. 2007; 25:989–1003. [PubMed: 17451904]

Wolbers T, Weiller C, Buchel C. Contralateral coding of imagined body parts in the superior parietal lobe. Cerebral Cortex. 2003; 13:392–399. [PubMed: 12631568]

Yoo SS, Fairneny T, Chen NK, Choo SE, Panych LP, Park H, Lee SY, Jolesz FA. Brain-computer interface using fMRI: spatial navigation by thoughts. Neuroreport. 2004; 15:1591–1595. [PubMed: 15232289]

Yoo SS, Jolesz FA. Functional MRI for neurofeedback: feasibility study on a hand motor task. Neuroreport. 2002; 13:1377–1381. [PubMed: 12167756]

Yoo SS, Lee JH, O'Leary H, Panych LP, Jolesz FA. Neurofeedback fMRI-mediated learning and consolidation of regional brain activation during motor imagery. International Journal of Imaging Systems and Technology. 2008; 18:69–78. [PubMed: 19526048]

Yoo SS, O'Leary HM, Lee JH, Chen NK, Panych LP, Jolesz FA. Reproducibility of trial-based functional MRI on motor imagery. International Journal of Neuroscience. 2007; 117:215–227. [PubMed: 17365109]

Yousry TA, Schmid UD, Alkadhi H, Schmidt D, Peraud A, Buettner A, Winkler P. Localization of the motor hand area to a knob on the precentral gyrus - A new landmark. Brain. 1997; 120:141–157. [PubMed: 9055804]

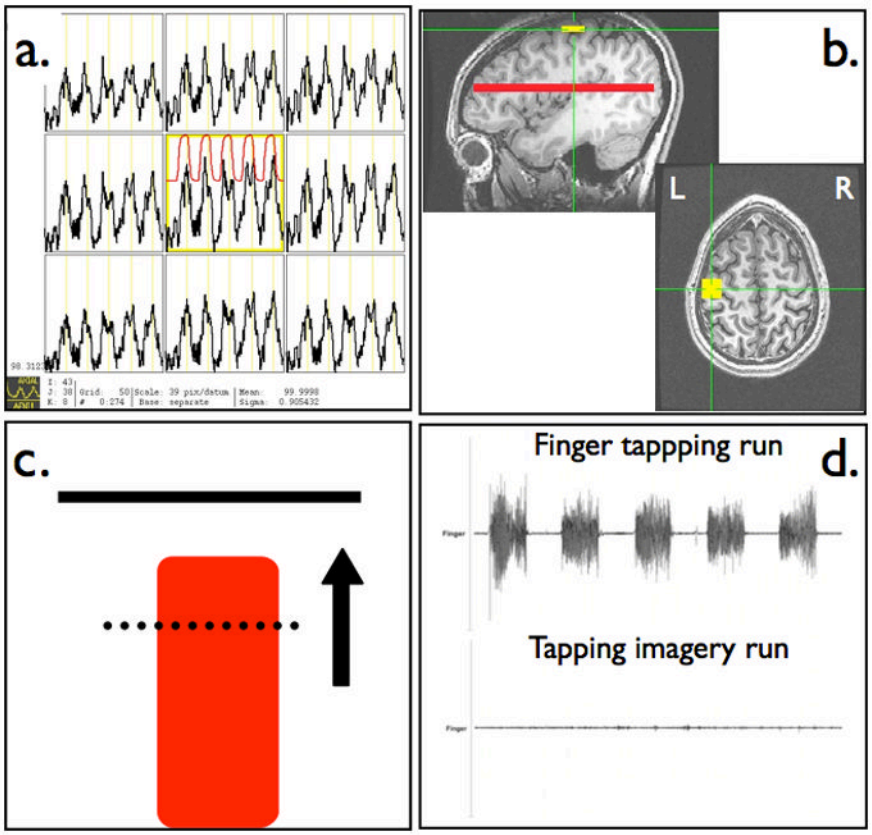

Figure 1.
Real-time fMRI scanning protocol with (a) continuously updated BOLD time series used for functional localization of primary motor cortex, (b) placement of square primary motor cortex ROI and whole brain axial slice for a reference ROI, (c) continuously updated neurofeedback display reflecting scan-to-scan level of BOLD signal within motor cortex ROI, and (d) monitoring of muscle movement during finger tapping and motor imagery neurofeedback tasks.

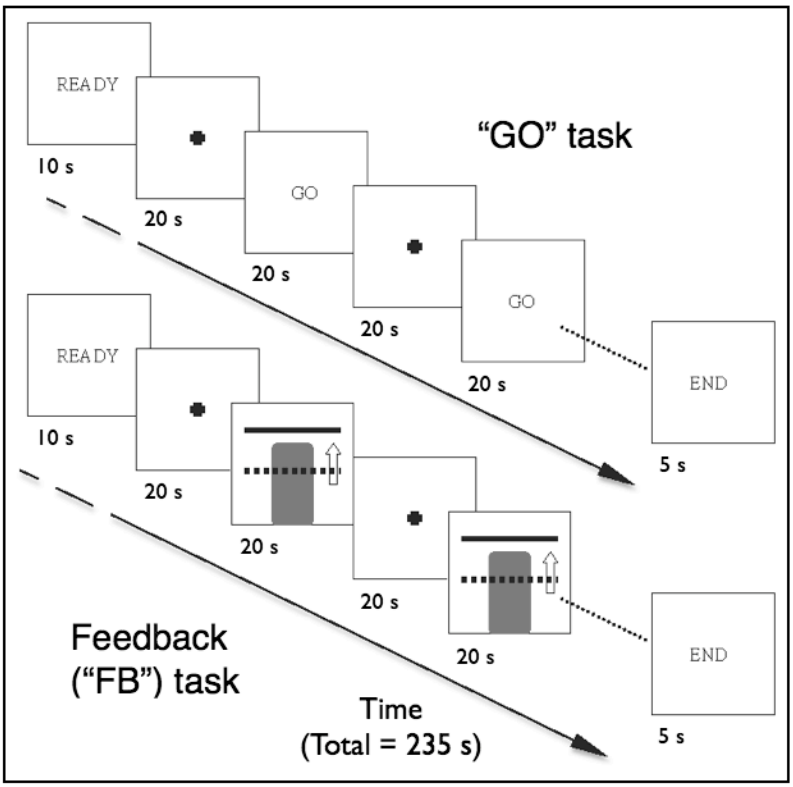

Figure 2.
RtfMRI-neurofeedback task paradigms showing the alternating 20 sec rest and active conditions during the GO and FB task runs.

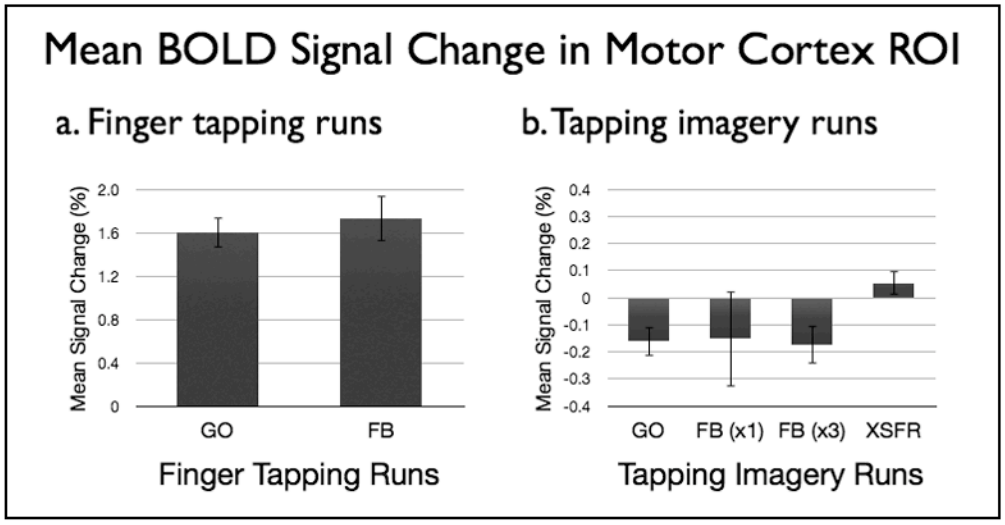

Figure 3.

Mean percent BOLD signal change from baseline within ROI_m during GO and FB runs with (a) finger tapping and (b) tapping imagery tasks. Subjects saw the neurofeedback display only during FB runs. Six subjects performed only one imagery FB run while nine subjects performed three imagery FB runs. All subjects (N=15) performed a tapping imagery XSFR run after NF training. Standard error of the mean is shown.

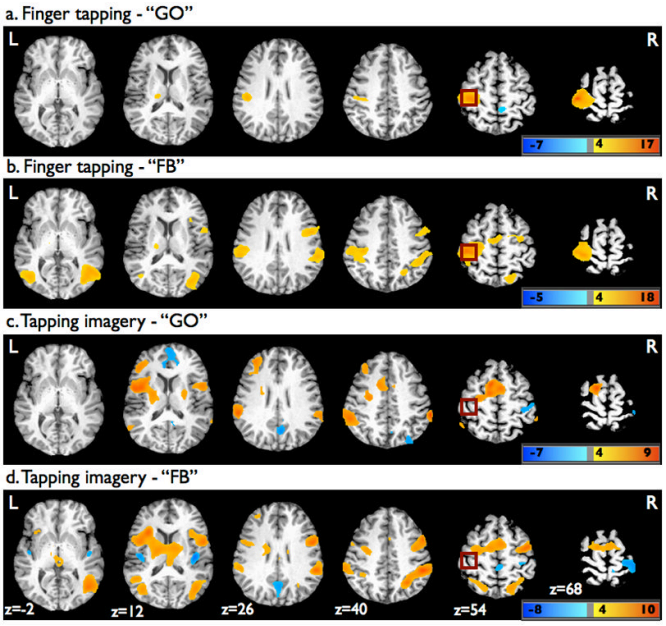

Figure 4.

Superimposed statistical parametric maps on axial brain slices of one participant's brain showing significant activation changes from baseline during the finger tapping (a) GO and (b) FB tasks, as well as the tapping imagery (c) GO and (d) FB tasks. For display purpose, the parametric maps were thresholded at p=0.001 (uncorrected) using a voxel cluster size threshold of 50 voxels. Dark red square shows approximate location of ROI_m.

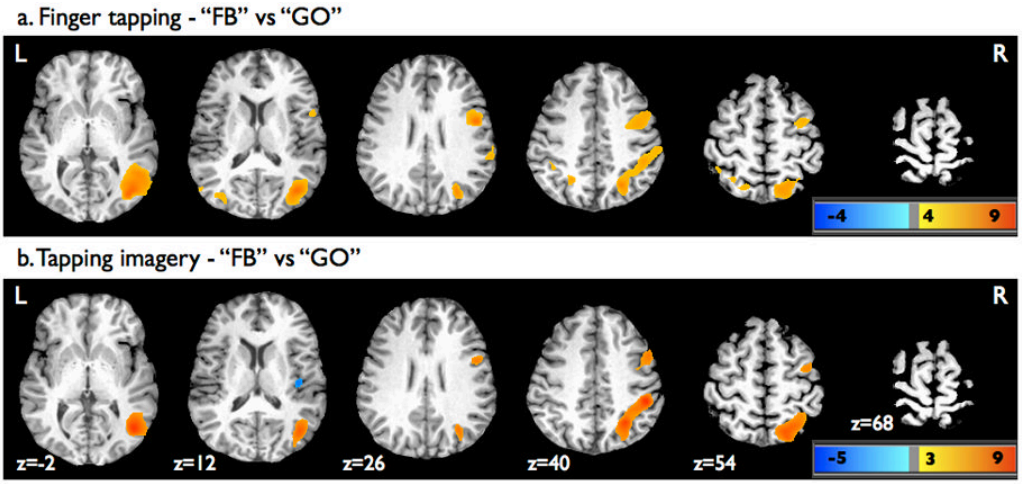

Figure 5.

Superimposed statistical parametric maps on axial brain slices of one participant's brain showing significant activation from contrasts of FB versus GO (a) during finger tapping and (b) tapping imagery. For display purpose, the parametric maps were thresholded at p=0.001 (uncorrected) using a voxel cluster size threshold of 50 voxels.

Table 1

Brain areas with significant activation changes during tapping and tapping imagery with and without neurofeedback

Task	Cluster size (mm^3)	Side	Region (Brodmann area)	Talairach coordinates X	Y	Z	Peak *t* value
Finger tapping							
GO	836	L	Precentral (4) and postcentral gyrus (1,2,3), inferior parietal lobe (40)	−43	−25	68	17.21
	79	R	Paracentral lobule (5)	11	−40	56	−6.69
	52	L	Thalamus	−16	−22	11	6.06
FB	1974	L	Precentral (4) and postcentral gyrus (1,2,3), medial frontal gyrus (6), inferior parietal lobe (40)	−16	−22	11	17.86
		R	Medial frontal gyrus (6), precental gyrus/middle frontal gyrus (6), inferior frontal gyrus (44)				
	1383	R	Middle occipital gyrus/middle temporal gyrus (19, 37), superior parietal lobe/precuneus (7), intraparietal sulcus, inferior parietal lobe (40)	38	−67	8	11.54
	258	L	Middle occipital gyrus/middle temporal gyrus (19, 37)	−43	−61	2	10.83
	74	L	Thalamus	−16	−19	11	5.52
Tapping imagery							
GO	895	L	Insula (anterior), putamen, middle frontal gyrus (8, 9)	−40	2	14	6.69
	750	L	Superior frontal gyrus (6), medial frontal gyrus (6), anterior cingulate cortex (ventral) (24), middle frontal gyrus/precentral gyrus (6)	−7	8	56	7.14
		R	Medial frontal gyrus (6), anterior cingulate cortex (ventral) (24)				
	480	L	Inferior parietal lobe (40)	−58	−34	29	7.13
	308	R	Putamen, precentral gyrus (6)	26	−10	5	6.19
	304	R	Postcentral gyrus (1, 2, 3)	41	−34	62	−6.66
	251	R/L	Anterior cingulate cortex (dorsal) (32), medial frontal gyrus (9, 10)	8	32	14	−6.70
	236	R>L	Posterior cingulate/precuneus (31, 7)	5	−61	26	−5.34
	234	R	Inferior parietal lobe (40)	65	−37	38	9.34
	192	R>L	Paracentral lobule/precuneus (5, 7)	8	−43	62	−5.74
	85	R	Precuneus (19)	32	−73	38	−4.86
FB	1563	R	Superior parietal lobe/precuneus (7), intraparietal sulcus, inferior parietal lobe (40), middle occipital gyrus/ middle temporal gyrus (19, 37)	23	−73	53	10.28
	1499	L	Insula (anterior), thalamus	−28	20	14	8.47
		R	Thalamus				

Task	Cluster size (mm^3)	Side	Region (Brodmann area)	Talairach coordinates			Peak *t* value
				X	Y	Z	
	1334	R	Middle frontal gyrus/precentral gyrus (6, 9), medial frontal gyrus (6), inferior frontal gyrus (44)	50	−1	53	8.69
		L	Middle frontal gyrus/precentral gyrus (6, 9), medial frontal gyrus (6)				
	287	L	Middle occipital gyrus/middle temporal gyrus (19, 37)	−40	−64	8	7.60
	268	L	Superior parietal lobe/precuneus (7), inferior parietal lobe (40)	−16	−61	53	6.41
	198	L	Inferior parietal lobe (40)	−55	−34	32	8.17
	106	L	Postcentral gyrus (1, 2, 3)	38	−28	65	−5.82
	86	R	Insula (posterior)	41	−16	8	−7.17
	64	L	Insula (posterior)	−43	−13	2	−7.77
	54	L	Superior frontal gyrus (9)	−34	41	32	6.09

Table 2

Brain activations associated with neurofeedback during motor and motor imagery tasks

Task	Cluster size (mm^3)	Side	Region (Brodmann area)	Talairach coordinates			Peak *t* value
				X	Y	Z	
Finger tapping							
FB vs GO	1279	R	Middle occipital gyrus/middle temporal gyrus (19, 37), superior parietal lobe/precuneus (7), intraparietal sulcus, inferior parietal lobe (40)	38	−70	8	8.89
	457	R	Precental gyrus/middle frontal gyrus (6), inferior frontal gyrus (44), insula (anterior)	50	2	20	6.43
	200	L	Middle occipital gyrus/middle temporal gyrus (19, 37)	−37	−61	2	6.86
	75	L	Superior parietal lobe/precuneus (7)	−22	−55	41	5.53
Tapping imagery							
FB vs GO	2022	R	Middle occipital gyrus/middle temporal gyrus (19, 37), superior parietal lobe/precuneus (7), intraparietal sulcus, inferior parietal lobe (40)	23	−73	53	8.77
	497	R	Precental gyrus/middle frontal gyrus (6, 9), inferior frontal gyrus (44)	50	5	32	5.57
	249	R	Thalamus	5	−34	2	4.58
	196	L	Middle occipital gyrus (19, 37)	−40	−64	5	5.41
	149	L	Superior parietal lobe/precuneus (7)	−22	−58	53	4.52